

Separation of motional processes in a [2]catenane by combining synthetic, dual-frequency EPR and molecular modelling approaches[†]

A. Godt¹ and G. Jeschke^{2*}

¹ Universität Bielefeld, Fakultät für Chemie, Universitätsstraße 25, 33615 Bielefeld, Germany

² Max Planck Institute for Polymer Research, Postfach 3148, 55021 Mainz, Germany

Received 31 March 2005; Revised 16 June 2005; Accepted 16 June 2005

Continuous-wave EPR of nitroxide spin labels at conventional (9.4 GHz) and high (94.2 GHz) frequencies is applied to characterize molecular dynamics in [2]catenanes composed of macrocycles with rigid phenyleneethynylene and flexible alkyl chain building blocks. By using a set of compounds with increasing complexity, which were all labelled at the centre of a rigid building block, it was possible to find regimes where spectral lineshapes were dominated by local motion of the spin label or those that contained information on tumbling of the building blocks. In chloroform, the macrocycles do not move as rigid objects, rather the rigid building block can reorient with some ease, with respect to the rest of the molecule. Furthermore, in that solvent the [2]catenane samples the co-conformational space on a timescale of microseconds or shorter. In a mechanical picture, chloroform can thus be considered as an effective lubricant that prevents the macrocycles from sticking together. Copyright © 2005 John Wiley & Sons, Ltd.

KEYWORDS: EPR; nitroxide spin labels; molecular dynamics; macrocycles; catenanes; molecular devices

INTRODUCTION

Ideas for nanostructured functional materials are often based on analogies to macroscopic or microscopic electrical and mechanical devices.^{1–5} In particular, proposed toolboxes of molecules and supramolecular assemblies for nanomechanical purposes imitate sets of simple geometrical objects, such as rings and cylinders. To what extent such analogies extend into nanoscopic dimensions is a matter of debate, since interactions between molecules have different relative magnitudes and a different scaling behaviour with distance than interactions between macroscopic objects. In addition, even shape-persistent molecules are usually much more flexible than the units of macroscopic mechanical devices.⁶ To learn about the mechanical behaviour of real molecular assemblies, such as [2]catenanes,⁷ methods are required that give information about the geometry and the dynamics of the molecular assemblies. As magnetic resonance techniques such as solid-state NMR⁸ and spin-label EPR⁹ can provide detailed information on molecular dynamics (MD) in soft matter, they appear as good candidates for such studies. For large, complex assemblies, labelling approaches may be more suitable.

In a recent study, we have demonstrated by pulse EPR measurements of distance distributions^{10–12} that the two concatenated macrocycles of certain [2]catenanes can be approximated as circular rings and that they populate uniformly all possible co-conformations, i.e. all possible relative orientations.¹³ Furthermore, we found that the macrocycles are largely expanded in chloroform. For the medium-sized [2]catenane 3c we find an experimental inner diameter of 3 nm for the macrocycles, which is much larger than the thickness of an alkyl chain or of a phenyleneethynylene unit. This suggests that the two macrocycles move rather unhindered, relative to each other. However, such measurements of distance distributions have to be performed at low temperatures in frozen solutions. Hence, they cannot provide an estimate for the timescale of this relative motion. We do know that the co-conformational distribution may change during the few minutes that it takes to dissolve and shock-freeze a sample, as we find different distance distributions when using *o*-terphenyl (OTP) or chloroform as the solvent.¹³ We also know that the proximity and relative motion of the macrocycles in these [2]catenanes do not manifest themselves in high-resolution ¹H NMR spectra¹⁴ or NOESY spectra. In the present study, we try to obtain an estimate for the timescale of the relative motion in liquid solution by analysing spin-label dynamics for a singly labelled [2]catenane and line broadening due to the presence of an additional spin label in the second macrocycle of a [2]catenane.

Such an estimate of the timescale can only be obtained from a rather detailed analysis of spin-label dynamics, as for

[†]Presented as part of a special issue on High-field EPR in Biology, Chemistry and Physics.

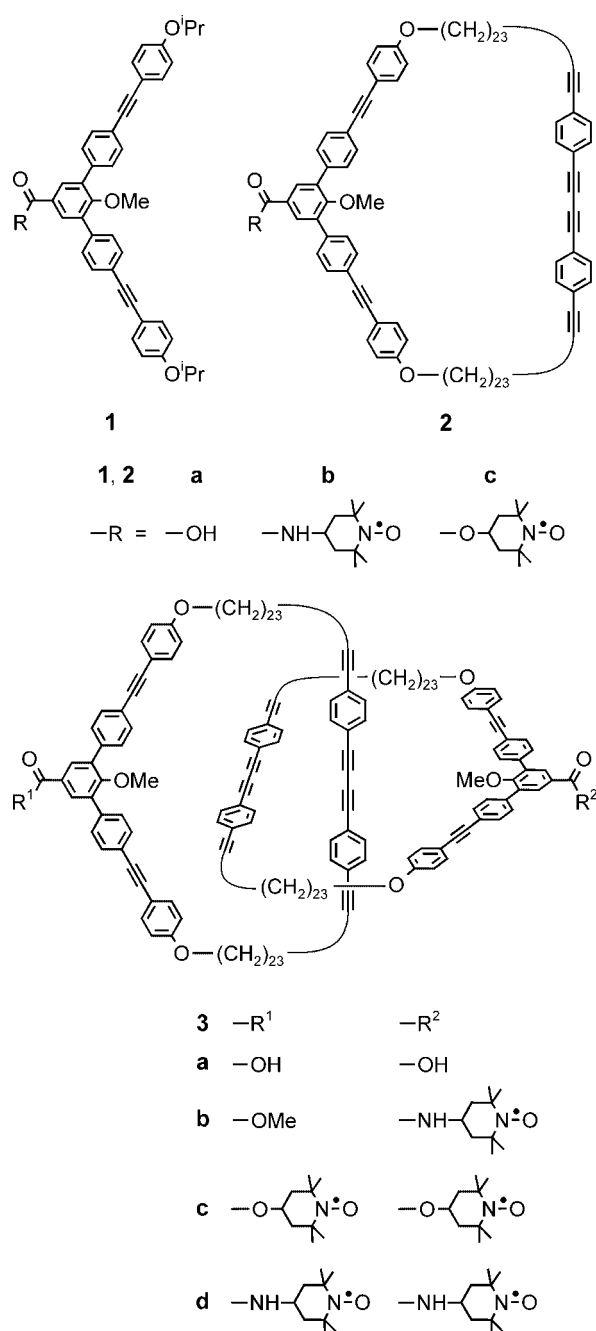
*Correspondence to: G. Jeschke, Max Planck Institute for Polymer Research, Postfach 3148, 55021 Mainz, Germany.

E-mail: jeschke@mpip-mainz.mpg.de

Contract/grant sponsor: Deutsche Forschungsgemeinschaft;

Contract/grant number: SPP 1051 (Hochfeld-EPR).

a spin label attached to a macromolecule several motional modes are superimposed.^{15,16} The present paper thus also has a methodological aspect, namely, the separation of contributions of local spin-label dynamics from those of global tumbling. This problem is approached by synthesizing a set of structurally related spin-labelled compounds that introduce additional influences on the nitroxide spectra step by step (Scheme 1). On the basis of this set of compounds, it is then tested whether variations in temperature, matrix viscosity, and microwave frequency can reliably help discriminate between the motional modes. To differentiate between the global motion of the [2]catenane and the relative motion of the two macrocycles, we compare the spectra of singly and doubly labelled [2]catenanes.



Scheme 1. Structural formulae of the investigated compounds.

RESULTS AND DISCUSSION

Strategy for separating motional modes

Perhaps even more than high-resolution NMR spectroscopy, EPR spectroscopy of slowly tumbling spin labels has revealed the high complexity of macromolecular dynamics in solution.⁹ Two main approaches for analysis of the spectra were developed in recent years. The first one, advanced mainly by the Freed group, heuristically tries to find the minimum number of superimposed motions that are required to fit the observed one- and two-dimensional spectra of nitroxide spin labels.^{15,16} The second approach, developed independently by Steinhoff and Hubbell¹⁷ as well as by Levine's group,¹⁸ uses the EPR spectra to decide to what extent a MD simulation of the macromolecule is in agreement with experimental observations. For the case at hand, both approaches have drawbacks. To incorporate relative motion of the two macrocycles of a [2]catenane into the model of slowly relaxing local structure¹⁶ and to validate this approach would be very tedious. MD simulations would have to include a solvent box. Because of computation time limitations they would not be able to extend to the timescale on which the two macrocycles move with respect to each other.

To reduce complexity of the problem, we try to identify regimes in which motion can be described by simpler models. Generally, motion of a label attached to a macromolecule can be described as a superposition of a local tether motion, local backbone fluctuations, and global tumbling (Fig. 1(a)). As in our compounds, the backbone in the vicinity of the label is rigid (Scheme 1), local backbone fluctuations are small and therefore do not make a significant contribution to rotational diffusion of the spin label. There should thus be a regime at relatively low temperatures or high viscosity of the matrix where rotational diffusion on the timescale of the EPR experiment (tens of picoseconds to microseconds) is dominated by tether motion. At higher temperatures and lower viscosity, tether motion is fast on the EPR timescale. As tether motion is restricted, it does not lead to complete averaging of the anisotropic contributions. In this regime, the lineshape is thus expected to be sensitive to tumbling of the angular rigid unit (partial tumbling) or even the whole molecule (global tumbling), Fig. 1(b–d). To check these ideas and obtain estimates on the rate of tumbling, we use compounds **1b**, **2b**, and **3b**. Within this set of compounds, local structure in the vicinity of the spin label, and hence tether motion, are the same, while the size of the macromolecule, and hence the rate of tumbling, change (Fig. 1(b–d)). By comparing compound **2b** to compound **1b**, we can ascertain whether or not the rate of tumbling influences the spectra and what components of the rotational diffusion tensor are affected. By comparing compound **3b** to compound **2b**, we can detect the influence of the concatenation restraint on the motion of the labelled macrocycle. Information on the rotational diffusion of the spin label in compound **3b** can then be used to discuss line broadening introduced by the presence of a second spin label in compound **3d**. The type and extent of this line broadening should, in turn, provide information on the relative motion of the two macrocycles.

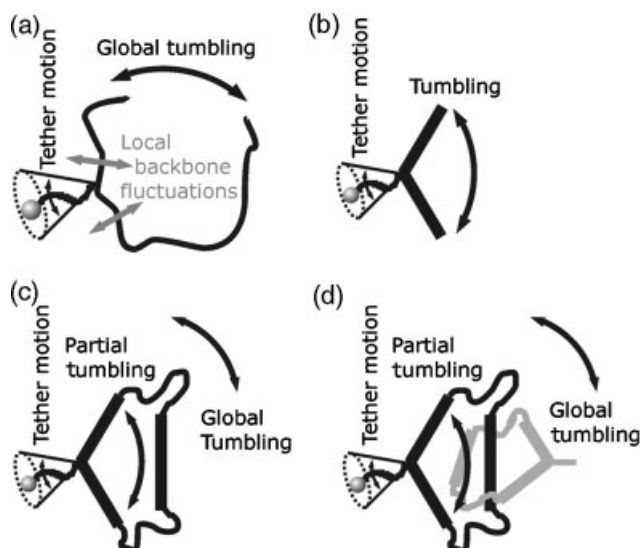


Figure 1. Motional modes expected for nitroxides (grey balls) attached to macromolecules. (a) General case. (b) Label attached to an angular rigid building block as in compound **1b**. (c) Label attached to a macrocycle composed of rigid and flexible building blocks as in compound **2b**. Tumbling of the angular unit may require tumbling of the rest of the molecule. (d) Label attached to a [2]catenane as in compound **3b**. Tumbling of the angular unit maybe further hindered by concatenation with the second macrocycle (grey).

High viscosity – EPR spectra dominated by tether motion

Compounds **1b**, **c**, **2b**, **3b–d** are well soluble in the glass former OTP as well as in the low-viscosity solvent chloroform. In OTP, at temperatures between the glass transition temperature of 244 K and approximately the melting point of 333 K, global motion is expected to have rotational correlation times longer than 1 μ s, so that it does

not significantly influence EPR spectra of nitroxides. Indeed, we observe such behaviour at 330 K at both X-band (9.4 GHz) and W-band (94.2 GHz) frequencies (Fig. 2). There are no significant differences between the spectra of compounds **1b**, **2b**, and **3b** except for a minor phase mismatch in the W-band measurement of compound **2b**. The small narrow features at 337.7 mT in the X-band spectra and 3354 mT in the W-band spectra are caused by less than 0.1% of free spin label. Remarkably, in the X-band spectra, tether motion is in the fast, rather than the slow, regime under conditions where global tumbling is still insignificant. This is manifested in the spectra in Fig. 2(a–c) by the appearance of three relatively narrow lines that can be assigned to the ^{14}N magnetic quantum numbers +1, 0, and –1.

As the precursor compounds are carboxylic acids, labels can be attached via an ester¹³ or amide linkage. Spectra of amide **1b** and its ester analog **1c** measured in OTP at 313 K at both X- and W-band look simpler for the amide than the ester linkage (Fig. 3). A MD simulation reveals why this is the case: on the timescale of EPR experiments, the ester interconverts between an *E*- and a *Z*-conformation, while the amide does not. Surprisingly, the bimodal nature of the tether motion for the ester linkage is more easily detected in the X-band spectrum (arrows in Fig. 3(d)). To avoid the complication of a bimodal tether motion, all other experiments were performed on compounds with the amide linkage. We did not attempt to obtain lineshape fits for the spectra shown in Fig. 3(c) and (e), as a detailed understanding of tether motion is not the aim of this work.

Low viscosity – extent of averaging limited by global tumbling

In a low-viscosity solvent at high temperature global tumbling of macromolecules with a size of a few nanometers is expected to proceed with correlation times in the nanosecond range or even shorter, i.e. on timescales where

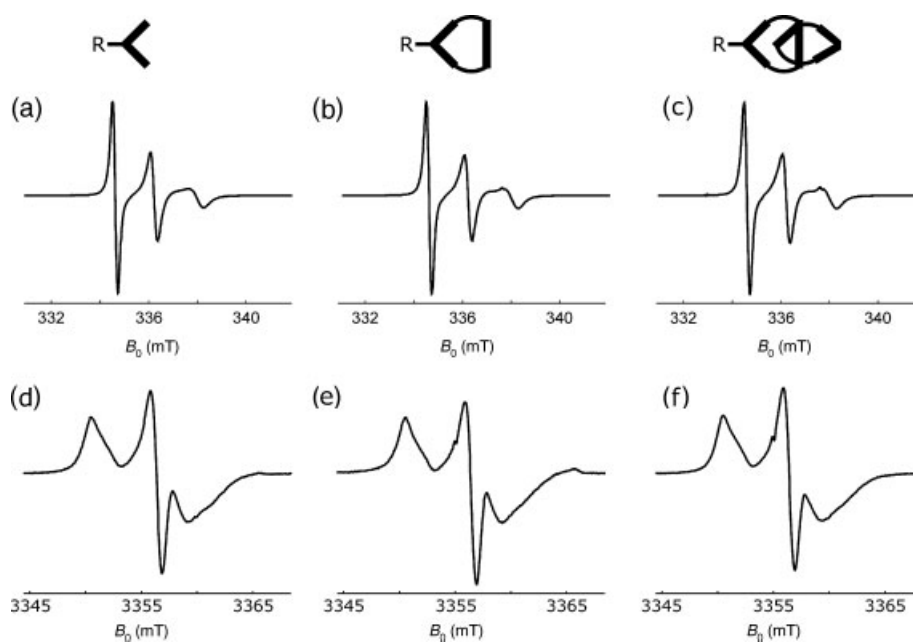


Figure 2. CW EPR spectra of compounds **1b**, **2b**, and **3b** in *o*-terphenyl at 330 K and 9.4 GHz (a–c) and 94.2 GHz (d–f). (a,d) Angular compound **1b**. (b,e) Macrocycle **2b**. (c,f) Singly labelled [2]catenane **3b**.

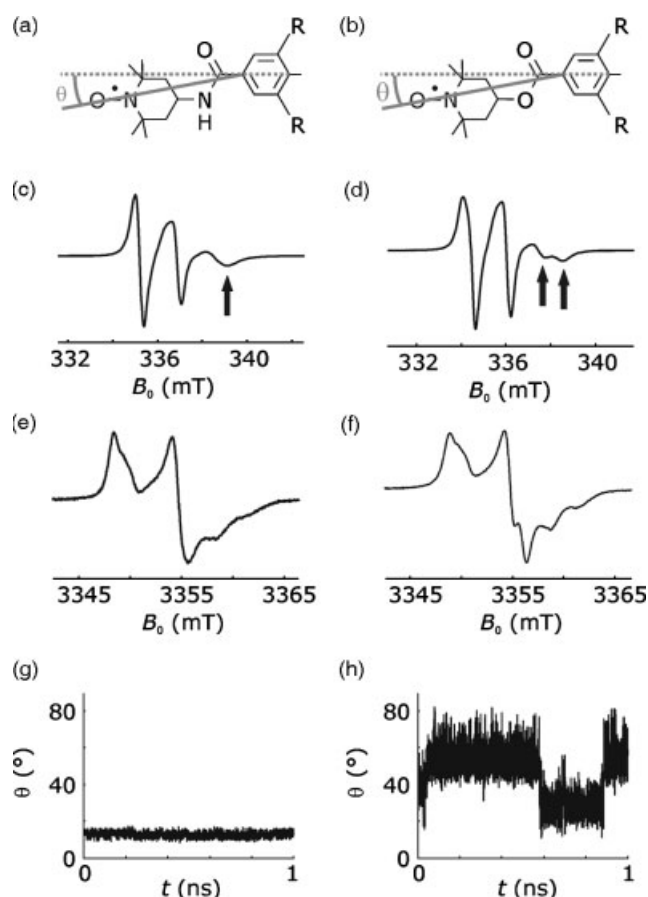


Figure 3. Comparison of label attachment via an amide linkage or ester linkage through studies on compound **1b** (left) and compound **1c** (right). (a,b) Tether structure and definition of cone angle θ . (c,d) CW EPR spectra in *o*-terphenyl at 9.4 GHz and 313 K. (e,f) CW EPR spectra in *o*-terphenyl at 94.2 GHz and 313 K. (g,h) Variation of θ in a molecular dynamics simulation in vacuum at 313 K.

nitroxide lineshapes are influenced. For our compounds, chloroform appears to be best suited, as measurements of the distance distribution in doubly labelled [2]catenanes **3c** indicated that the macrocycles are expanded in this solvent and adopt all possible co-conformations.¹³ For the diamide **3d**, we found the same distance distribution as for the diester **3c** (data not shown). As Continuous-wave EPR (CW EPR) linewidths were found to decrease significantly with increasing temperature, we performed the measurements at the highest possible temperature of 325 K (boiling point of chloroform: 334 K). In this regime, we find clearly visible differences between the spectra of angular compound **1b** and macrocycle **2b** (compare Fig. 4(a) with (b) and 5(d) with (e)) and slight differences between the latter and the singly labelled [2]catenane **3b** (compare Fig. 4(b) with (c) and 5(e) with (f)). This indicates that concatenation does not strongly constrain motion of the macrocycle.

To quantify the differences, we fitted the spectra with the simplest motional model that could account for the lineshapes. We found that a model of isotropic Brownian rotational diffusion could not reproduce the relative amplitudes of the three lines for any of the compounds (data not shown). Likewise, the rotational correlation times $\tau_{c'}'$, $\tau_{c'}''$, and $\tau_{c'}'''$ computed from the amplitude ratios and linewidths by the three expressions given by Buchachenko *et al.*¹⁹ do not agree, as they should for isotropic rotary diffusion. Good fits of the X-band data (for example, Fig. 5(a, e)) are obtained with a model of uniaxial anisotropic rotary diffusion with the unique axis being the *y*-axis of the molecular frame. This axis is perpendicular to both the N–O bond and the p_π orbital lobes on the nitrogen atom. As discussed by Buchachenko *et al.*,¹⁹ a reliable assignment of the unique axis may not be possible in the regime of fast uniaxial rotary diffusion. Furthermore, the spectra are rather insensitive to the principal value R_{\parallel} of the rotational diffusion tensor along the unique axis. It is also clear that the actual motion is a superposition of fast partial averaging by tether motion and slower

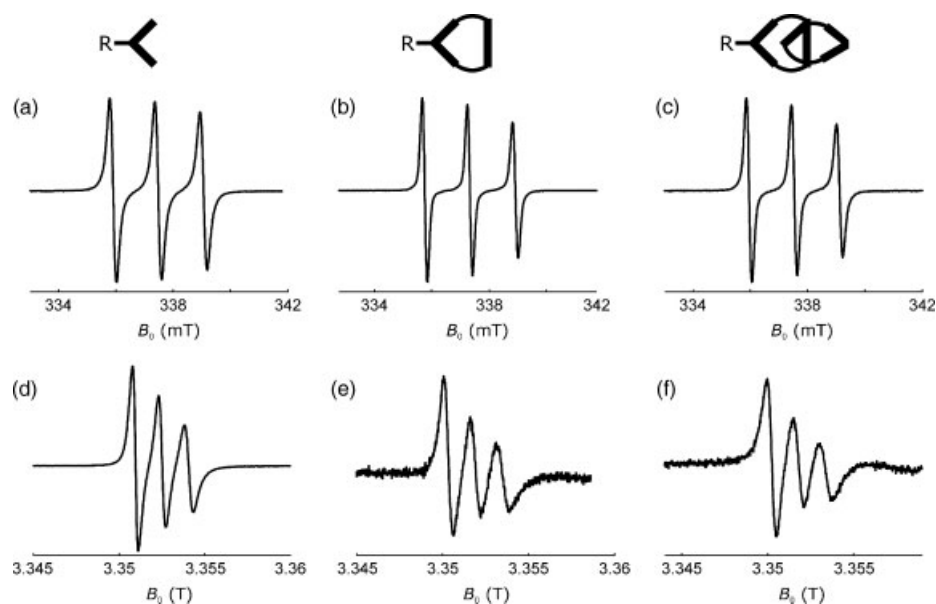


Figure 4. CW EPR spectra of compounds **1b**, **2b**, and **3b** in chloroform at 325 K and 9.4 GHz (a–c) and 94.2 GHz (d–f). (a,d) Angular compound **1b**. (b,e) Macrocycle **2b**. (c,f) singly labelled [2]catenane **3b**.

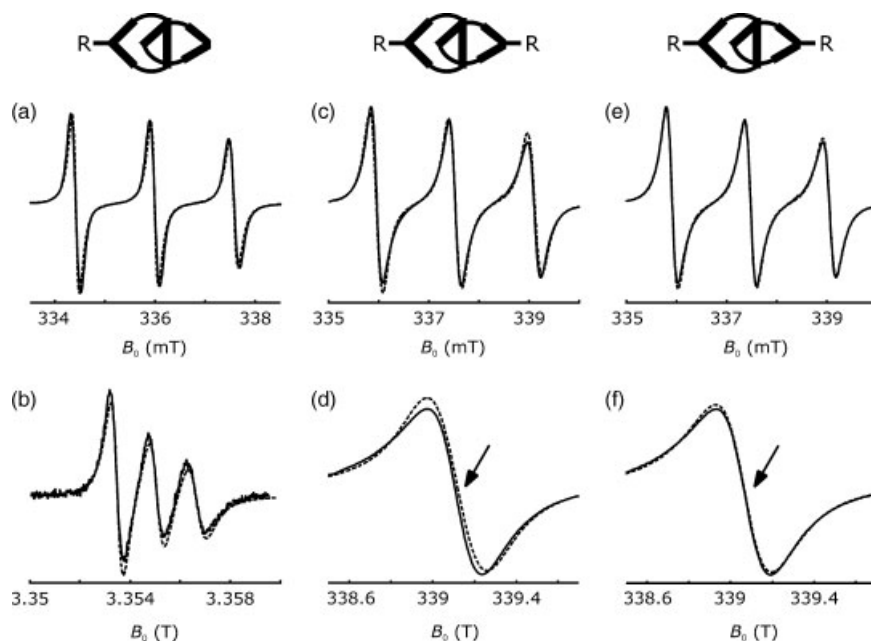


Figure 5. Analysis of line broadening due to the presence of a second label in [2]catenane **3d** compared to singly labelled [2]catenane **3b** (chloroform, 325 K). Solid lines are experimental spectra; dashed lines are best fits. (a) Spectrum of [2]catenane **3b** at 9.4 GHz, fit with uniaxial anisotropic rotational diffusion, $R_{\perp} = 0.5 \times 10^9 \text{ s}^{-1}$, $R_{\parallel} = 4 \times 10^{11} \text{ s}^{-1}$. (b) Spectrum of [2]catenane **3b** at 94.2 GHz, fit with uniaxial anisotropic rotational diffusion, same parameters as in (a). (c) Spectrum of [2]catenane **3d** at 9.4 GHz, fit by convolution of the spectrum in (a) with a Lorentzian. (d) High-field detail of (c). The experimental line is shifted to low-field with respect to the simulation (arrow). (e) Spectrum of [2]catenane **3d** at 9.4 GHz, fit with uniaxial anisotropic rotational diffusion, $R_{\perp} = 0.4 \times 10^9 \text{ s}^{-1}$, $R_{\parallel} = 4 \times 10^{11} \text{ s}^{-1}$ and a Heisenberg exchange frequency of 20 MHz. (f) High-field detail of (e). The field positions of the experimental line and simulated lines coincide (arrow).

isotropization by global tumbling of the molecule. In this situation, the principal value R_{\perp} that is perpendicular to the unique axis can be considered as a rough estimate of the timescale of global tumbling. This value is also found to depend on temperature (data not shown). We have obtained R_{\perp} values for all compounds at 325 K in chloroform by fits of X-band and W-band spectra with the Schneider/Freed program package.¹⁵

An overview of these data is given in Table 1. Because of slight phase errors in the experimental spectra, fits are slightly worse at W-band frequencies (e.g., Fig. 5(b)), so that the values obtained from those spectra are less reliable. As the purpose of this analysis is only a timescale *estimate*, we may conclude that the data at the two frequencies agree reasonably well. As expected, R_{\perp} decreases with increasing size of the molecule. The value for the singly labelled [2]catenane **3b** is significantly smaller than the one for the macrocycle **2b**, which implies that the concatenation constraint influences rotational diffusion of the label. We may roughly estimate the increase of an effective rotational radius r_{eff} of the molecules by using the Stokes–Einstein relation.

Table 1. Perpendicular component of axial rotational diffusion tensors obtained from fitting spectra of compounds **1b**, **2b**, **3b**, **d** in chloroform at 325 K at 9.4 GHz ($R_{\perp,X}$) and 94.2 GHz ($R_{\perp,W}$)

Compound	1b	2b	3b	3d
$R_{\perp,X}/10^9 \text{ s}^{-1}$	0.85 ± 0.1	0.675 ± 0.1	0.5 ± 0.05	0.4 ± 0.05
$R_{\perp,W}/10^9 \text{ s}^{-1}$	0.85 ± 0.2	0.55 ± 0.15	0.5 ± 0.05	0.5 ± 0.05

According to this relation, which is strictly valid only for rotational diffusion of a sphere, R_{\perp} should scale with r_{eff}^{-3} . Hence, the effective rotational radius for the macrocycle **2b** is only by a factor of 1.08 larger than for the rigid angular building block **1b**. The concatenation constraint increases the effective radius by another factor of 1.1. These small changes indicate that because of the flexible alkyl chains, tumbling of the angular building block is only weakly coupled to tumbling of the whole molecule. In other words, neither the macrocycle nor the [2]catenane tumble like a rigid object. The relative motion of the building blocks is significant at 325 K on a nanosecond timescale. The same is also true at ambient temperature.

We can also safely conclude that the rotational correlation time about any axis is shorter than 1 ns for all compounds. Together with the planar extension of the rigid angular unit ($1.2 \times 2.4 \text{ nm}^2$), this implies that the label traces a volume of more than 5 nm^3 on a nanosecond timescale. This, in turn, means that the distance vector between the two labels in compound **3d** also rotates on this timescale. Any residual dipole–dipole coupling between the two labels is thus expected to be much smaller than the linewidths of approximately 6 MHz observed at X-band for the singly labelled [2]catenane **3b**.

Line broadening in the doubly labelled [2]catenane – relative motion of the macrocycles

The only difference between compounds **3b** and **3d** is the introduction of a second spin label at a site of the concatenated ring that is equivalent to the site of

the first spin label. In the W-band spectra, where the linewidths for compound **3b** are larger than 15 MHz, this does not cause significant changes. However, in the X-band spectra significant additional broadening is observed for the doubly labelled compound **3d** (compare Fig. 5(c) to (a)). As concluded in the previous section, because of the fast motion this broadening cannot be due to residual dipole–dipole couplings. Possible sources are a decrease in the transverse relaxation time T_2 due to dipolar relaxation and exchange broadening. Dipolar relaxation can be simulated by convolution of the experimental absorption spectrum (integrated CW EPR spectrum) of the singly labelled [2]catenane **3b** with a Lorentzian line and pseudomodulation to obtain again a first-derivative spectrum. The width of the Lorentzian line can be treated as a fit parameter. The best fit obtained by such a simulation is shown in Fig. 5(c), and a detailed plot of the high-field line in Fig. 5(d). Although the fit is not poor, one notices a small low-field shift of the experimental high-field line with respect to the simulated line (arrow in Fig. 5(d)). Similarly, a slight high-field shift of the low-field line is observed. In other words, the apparent hyperfine coupling is smaller for compound **3d** than for compound **3b**. Such a reduction in the apparent hyperfine coupling is expected for exchange coupling as a broadening mechanism.²⁰

Indeed, the best fit of the X-band spectrum of compound **3d** with the Schneider/Freed program¹⁵ including Heisenberg exchange is better than with simple convolution (Fig. 5(e, f)). The improvement in relative amplitudes of the lines is due to a slight change in R_{\perp} compared to that in compound **3b** (Table 1). However, the reduced hyperfine splitting is only reproduced if Heisenberg exchange is included. The fit yields an exchange frequency of 20 MHz. We cannot exclude that dipolar relaxation contributes to the broadening to some extent, but we can safely conclude that the reduction in the hyperfine splitting is not reproduced for exchange frequencies smaller than 10 MHz. This implies effective collisions of the two nitroxide labels on a submicrosecond timescale and as a result, relative motion of the two macrocycles in the [2]catenane on that timescale.

Finally, we have to consider whether this relative motion on the submicrosecond timescale samples the whole space of co-conformations. From measurements of the distance distribution, we know that in chloroform solutions of **3c**¹³ and **3d** the whole space of co-conformations is almost uniformly populated. If the timescales of nitroxide–nitroxide collisions and of sampling of the whole co-conformational space were significantly different, we would thus expect a *distribution* of exchange frequencies with fast exchange for co-conformational subensembles with short nitroxide–nitroxide distances and slow or no exchange for subensembles with long nitroxide–nitroxide distances. The occurrence of such subensembles with different exchange frequencies leads to lineshapes with broad wings and narrow centres, as we have recently observed for counterions near polyelectrolytes.²¹ Such lineshapes cannot be fitted by a single exchange frequency. In the present case, the lineshapes are well reproduced by a single exchange frequency, which implies that the timescales of nitroxide–nitroxide collisions

and of sampling the co-conformational distribution are not separated. We may thus conclude that the co-conformational space is sampled on a timescale of microseconds or less. It thus appears that in chloroform, the two macrocycles in [2]catenanes **3** move relatively unhindered with respect to each other; they are not sticky.

CONCLUSION

The dynamics of a [2]catenane composed of macrocycles with both rigid and flexible building blocks could be unravelled by analysing CW EPR lineshapes of nitroxide spin labels attached to one or both of the angular rigid building blocks. Tethering of the spin label via an amide linkage gave simpler spectra than tethering via an ester linkage. A small increase in the rotational correlation time when going from just the angular building block to a macrocycle implies that the macrocycles do not move as rigid objects. Rather, the angular units can rotate considerably with respect to the rest of the molecule. Analysis of the line broadening imposed by attaching a second label to a [2]catenane reveals that the two macrocycles do not stick together in chloroform, and that they move freely with respect to each other on a microsecond timescale. To return to a macroscopic mechanical picture, this means that chloroform acts as an effective lubricant for molecules composed of phenyleneethynylene and alkyl chain building blocks.

The method described here may open a way to investigate entropy-driven nanomechanical devices on the basis of flexible molecular subunits that have been recently suggested by Hanke and Metzler.²²

EXPERIMENTAL

EPR spectroscopy

CW EPR at X-band frequencies of approximately 9.4 GHz was performed with a Bruker Elexsys 580 spectrometer equipped with a 4103 TM/0105 rectangular cavity and an ER 4111 variable temperature unit. A microwave power of 2 mW and a modulation amplitude of 0.05 mT were used. The sweep width was 20 mT for spectra measured in OTP (Fluka) matrix and 10 mT for spectra measured in chloroform (Fluka, stabilized with 1% ethanol) solution. In both cases, 2048 data points were acquired. CW EPR at W-band frequencies of approximately 94.2 GHz was performed with a Bruker Elexsys 680 spectrometer equipped with a Bruker ENDOR resonator and an Oxford cryostat for temperature control. Nitrogen gas was used as a heating medium. A microwave power of 0.05 mW and a modulation amplitude of 0.1 mT were used. The sweep width was 35 mT for spectra measured in OTP matrix and 15 mT for spectra measured in chloroform solution. In both cases, 1024 points were acquired.

All spectra were measured on samples with total label concentrations below 1 mmol l^{-1} , so that an influence of intermolecular Heisenberg exchange on lineshapes could be excluded. All samples were kept in the corresponding solvents and at the corresponding temperatures for a sufficient time to equilibrate with the oxygen from air. Control measurements of compound **1b** revealed that for

the used protonated spin labels in chloroform at ambient temperature, line broadening by oxygen is noticeable, though not dominant. Such broadening is not significant in chloroform at 325 K.

MD simulations

MD simulations were carried out with the program package Cerius 2 (v. 3.8, Molecular Simulations, Inc.), using the CFF91 force field. The systems were first pre-equilibrated (canonical ensemble in a Berendsen temperature bath, 20 000 steps, time step 0.5×10^{-15} s) and then sampled by a 1 ns run (Nosé-Hoover thermostat, 2×10^6 steps, time step 0.5×10^{-15} s). Structures were written to trajectory files in time intervals of 1×10^{-13} s. Time traces of the nitroxide and backbone coordinates were extracted from the trajectory files using the gOpenMol program and analysed by a home-written Matlab (The MathWorks, Inc.) program.

EPR spectrum simulations

CW EPR spectral simulations were performed with a program by Schneider and Freed assuming a uniaxial tensor of rotational diffusion.¹⁵ The following magnetic parameters were assumed: *g*-tensor: $g_{xx} = 2.0090$, $g_{yy} = 2.0060$, $g_{zz} = 2.0024$; hyperfine-tensor: $A_{xx} = 0.68$ mT, $A_{yy} = 0.62$ mT, $A_{zz} = 3.43$ mT. Within the precision of our approach, rotational correlation times do not depend on the small variations of these parameters with solvent polarity.

Preparation of spin-labelled compounds

General

All reactions were carried out under inert atmosphere in dried Schlenk flasks. THF was dried over sodium/benzophenone and piperidine over CaH_2 . CH_2Cl_2 and DMF were purchased in sealed bottles over molecular sieves. The diethyl ether that was used for workup and chromatography of the spin-labeled compounds was distilled from sodium prior to use to remove the stabilizer. The petroleum ether used had a boiling range of 30–40 °C. For flash chromatography, silica gel was used. The NMR spectra were recorded on a 300-MHz instrument at room temperature in CDCl_3 as solvent and internal standard. The assignment of the ^{13}C NMR signals is in accordance with DEPT-135 measurements. The subscripts α , β , γ , and δ refer to the aromatic rings. The hydroxybenzoate moiety is named α . The benzene unit closest to the hydroxybenzoate moiety is named β , the benzene unit connected with Ar_β by only one ethyne moiety is named γ , and the residual benzene unit is named δ . For the numbering of the positions, the ethyl 4-hydroxybenzoate is considered as the substituted parent compound. Melting points were determined in open capillaries.

Synthesis of acid 1a

Ethyl 3,5-di[4-(4-isopropoxyphenylethynyl)phenyl]-4-hydroxybenzoate (1d)

To a carefully degassed (freeze-pump-thaw method) solution of ethyl 3,5-di(4-ethynylphenyl)-4-hydroxybenzoate²³ (4.32 g, 11.8 mmol) and 1-isopropoxy-4-iodobenzene (1-Isopropoxy-4-iodobenzene was obtained from 4-iodophenol and 2-bromopropane in analogy to the preparation of 1-ethoxy-4-iodobenzene (Ref. 24). Distillation (77–83 °C/ 10^{-2} torr) gave the colorless, slowly solidifying product.) (7.42 g, 28.3 mmol) in piperidine (60 ml),

$\text{Pd}(\text{PPh}_3)_2\text{Cl}_2$ (85 mg, 0.12 mmol) and CuI (44 mg, 0.23 mmol) were added. Soon a precipitate formed. After 17 h at room temperature, the reaction mixture was diluted with CH_2Cl_2 , washed with 2 N HCl (exothermic) and the combined aqueous phases were extracted with CH_2Cl_2 . The combined organic phases were dried (Na_2SO_4) and concentrated in vacuo. Flash chromatography (petroleum ether/ CH_2Cl_2 1:2 v/v) gave **1d** containing a trace of 1-isopropoxy-4-iodobenzene. This material was dissolved in CH_2Cl_2 (15 ml), and **1d** (5.6 g, 74%) was precipitated through addition to petroleum ether (300 ml) as a colourless solid: m.p. = 167.2–169.3 °C; ^1H NMR: $\delta = 7.98$ (s, 2 H, H_α), 7.61 and 7.53 (AA'XX', 4 H each, H_β), 7.46 (half of AA'XX', 4 H, H_γ -2,-6), 6.85 (half of AA'XX', 4 H, H_γ -3,-5), 5.78 (s, 1 H, OH), 4.57 (sept, $J = 6.0$ Hz, 2 H, CHCH_3), 4.36 (q, $J = 7.1$ Hz, 2 H, CO_2CH_2), 1.37 (t, $J = 7.0$ Hz, 3 H, CH_2CH_3), 1.34 (d, $J = 6.0$ Hz, 6 H, CHCH_3); ^{13}C NMR: $\delta = 166.1$ (CO_2), 158.2 (C_γ -4), 153.2 (C_α -4), 135.9 (C_β -1), 133.1 (C_γ -2,-6), 132.0 (C_β -3,-5), 131.6 (C_α -2,-6), 129.3 (C_β -2,-6), 128.3 (C_α -3,-5), 123.7, 123.4 (C_α -1, C_β -4), 115.8 (C_γ -3,-5), 114.9 (C_γ -1), 90.6 ($\text{C}\equiv\text{C}_{\text{Ar}_\gamma}$), 87.6 ($\text{C}\equiv\text{C}_{\text{Ar}_\gamma}$), 70.0 (CHCH_3), 60.9 (CO_2CH_2), 22.0 (CHCH_3), 14.4 (CH_2CH_3).

Ethyl 3,5-di[4-(4-isopropoxyphenylethynyl)phenyl]-4-methoxybenzoate (1e)

A suspension of **1d** (3.01 g, 4.74 mmol), methyl iodide (0.6 ml, 9.6 mmol) and K_2CO_3 (1.3 g, 9.4 mmol) in DMF (80 ml) was stirred for 15 h at 40 °C. The reaction mixture was poured into water. The precipitate was isolated and washed well with water. Drying (P_4O_{10} , vacuum) gave **1e** (2.9 g, 94%) as a colourless solid. m.p. = 179.1–179.4 °C; ^1H NMR: $\delta = 8.04$ (s, 2 H, H_α -2,-6), 7.58 (apparent s, 8 H, H_β), 7.46 (half of AA'XX', 4 H, H_γ -2,-6), 6.85 (half of AA'XX', 4 H, H_γ -3,-5), 4.57 (sept, $J = 6.1$ Hz, 2 H, CHCH_3), 4.38 (q, $J = 7.1$ Hz, 2 H, CO_2CH_2), 3.21 (s, 3 H, OCH_3), 1.38 (t, $J = 6.1$ Hz, 3 H, CH_2CH_3), 1.33 (d, $J = 6.1$ Hz, 12 H, CHCH_3); ^{13}C NMR: $\delta = 166.0$ (CO_2), 158.8 (C_γ -4), 158.2 (C_α -4), 137.3, 135.2 (C_α -3,-5, C_β -1), 133.1 (C_γ -2,-6), 131.7 (C_α -2,-6), 131.4 (C_β -3,-5), 129.2 (C_β -2,-6), 126.5 (C_α -1), 123.0 (C_β -4), 115.8 (C_γ -3,-5), 115.0 (C_γ -1), 90.3 ($\text{C}\equiv\text{C}_{\text{Ar}_\gamma}$), 87.8 (Ar_β $\text{C}\equiv\text{C}$), 70.0 (CHCH_3), 61.1 (CO_2CH_2), 60.7 (OCH_3), 22.0 (CHCH_3), 14.4 (CH_2CH_3); elemental analysis (%) calculated for $\text{C}_{44}\text{H}_{40}\text{O}_5$ (648.799): C 81.46 H 6.21; found C 81.46, H 6.21.

3,5-Di[4-(4-isopropoxyphenylethynyl)phenyl]-4-methoxybenzoic acid (1a)

10 N NaOH (10 ml) was added to a suspension of **1e** (2.98 g, 4.70 mmol) in THF (50 ml) and ethanol (30 ml). Upon heating to 45 °C, the reaction mixture became a clear solution. After 16 h at 45 °C, the reaction mixture was cooled with an ice bath and the product **1a** (2.80 g, 98%) was precipitated through the addition of 2 N HCl as a colourless solid that was dried (P_4O_{10} , vacuum). m.p. = 232.1–233.0 °C; ^1H NMR: $\delta = 8.12$ (s, 2 H, H_α), 7.60 (apparent s, 8 H, H_β), 7.47 (half of AA'XX', 4 H, H_γ -2,-6), 6.86 (half of AA'XX', 4 H, H_γ -3,-5), 4.57 (sept, $J = 6.1$ Hz, 2 H, CHCH_3), 3.23 (s, 3 H, OCH_3), 1.34 (d, $J = 6.1$ Hz, 12 H, CHCH_3); ^{13}C NMR: $\delta = 171.4$ (CO_2), 159.7 (C_α -4), 158.1 (C_γ -4), 137.0, 135.4 (C_α -3,-5, C_β -1), 133.1 (C_γ -2,-6), 132.4 (C_α -2,-6), 131.4 (C_β -3,-5), 129.2 (C_β -2,-6), 125.2 (C_α -1), 123.1 (C_β -4), 115.8 (C_γ -3,-5), 115.0 (C_γ -1), 90.4 ($\text{C}\equiv\text{C}_{\text{Ar}_\gamma}$), 87.8 (Ar_β $\text{C}\equiv\text{C}$), 70.0 (CHCH_3), 60.7 (OCH_3), 22.0 (CHCH_3); elemental analysis (%) calculated for $\text{C}_{42}\text{H}_{36}\text{O}_5$ (620.745): C 81.27, H 5.85; found C 81.25, H 5.80.

Compound 1b (compound 1 labelled with 4-amino-TEMPO)

N-Hydroxysuccinimide (20 mg, 0.17 mmol) was added to a suspension of acid **1a** (99 mg, 0.16 mmol) in CH_2Cl_2 (3 ml). Upon addition of *N,N'*-dicyclohexylcarbodiimide (36 mg, 0.17 mmol) the suspension turned into a clear solution. Shortly after the solution became turbid, again. Then 4-amino-2,2,6,6-tetramethylpiperidinyloxy (4-amino-TEMPO; 40 mg, 0.23 mmol) was added. After stirring the reaction mixture at room temperature for 40 h, the precipitate was removed by filtration and washed with CH_2Cl_2 until it was colourless. Removal of the solvent from the filtrate gave a reddish solid. Chromatography using a chromatotron (petroleum ether/ CH_2Cl_2 1:1 v/v \rightarrow petroleum ether/ CH_2Cl_2 / Et_2O 15:15:1 \rightarrow 15:15:2 v/v/v) gave **1b** (79 mg, 64%) as a reddish solid. m.p. = 135 °C sintering with discoloration; ^1H NMR: all signals are broad. $\delta = 7.66$ (apparent s with shoulder at 7.9 ppm, > 2 H, H_β and H_α), 7.53 (half of AA'XX', 4 H, H_γ -2,-6), 6.93 (half of AA'XX', 4 H, H_γ -3,-5), 4.64 (t in outlines, 2 H, CHCH_3), 3.28 (s, 3 H, OCH_3), 1.41 (d, $J = 5.3$ Hz, 12 H, CHCH_3); elemental analysis (%) calculated for $\text{C}_{51}\text{H}_{53}\text{N}_2\text{O}_5$ (773.994): C 78.14, H 6.90, N 3.62; found C 78.53, H 6.86, N 3.57.

FD-MS: $m/z = 759.7$ (18%, $[M - \text{CH}_3]^+$), 775.5 (100%, M^+), 1535 (10%, $[2M - \text{CH}_3]^+$), 1549.4 (10%, $[2M]^+$).

Compound 1c (compound 1 labelled with 4-hydroxy-TEMPO)

The mixture of acid **1a** (80 mg, 0.13 mmol), 4-hydroxy-TEMPO (25 mg, 0.15 mmol), 4-(dimethylamino)pyridin (17 mg, 0.14 mmol) and *N*-ethyl-*N'*-(3-dimethylaminopropyl)carbodiimide hydrochloride (37 mg, 0.19 mmol) were dissolved in CH_2Cl_2 (4 ml). This solution was stirred at 45 °C for 14 h. After cooling to room temperature, diethyl ether and 2 N HCl were added. The aqueous phase was extracted with diethyl ether. The combined organic phases were washed with 2 N HCl and dried (MgSO_4) and the solvent was removed at reduced pressure. Flash chromatography (petroleum ether/diethyl ether 2:1 v/v; the compound was applied as a solution in CH_2Cl_2) gave **1c** (87 mg, 87%) contaminated with a small amount of acid **1a** (The sharp signal at 8.12 ppm (H_α) in the ^1H NMR spectrum and the signal at $m/z = 620.7$ (2%, $[M(\mathbf{1a})]^+$) in the mass spectrum proves the presence of acid **1a**. Because of ^1H NMR signal overlap the amount can only be estimated to be rather small.) as an orange-coloured solid (Based on our later results when working with 4-hydroxy-TEMPO labelled catenanes (Ref. 13) using a gradient petroleum ether/ $\text{CH}_2\text{Cl}_2 \rightarrow$ petroleum ether/ $\text{CH}_2\text{Cl}_2/\text{Et}_2\text{O}$ will most probably give pure compound **1c**). ^1H NMR: all signals are broad. $\delta = 8.2$ (very broad s, 2 H, H_α), 7.77 (apparent s, 8 H, H_β), 7.63 (half of AA'XX', the fine structure is hardly resolved 4 H, H_γ -2,-6), 7.03 (half of AA'XX', the fine structure is hardly resolved 4 H, H_γ -3,-5), 4.75 (m, 2 H, CHCH_3), 3.40 (s, 3 H, OCH_3), 1.52 (d, the fine structure is hardly resolved 12 H, CHCH_3); $\text{C}_{51}\text{H}_{52}\text{NO}_6$ (774.978): FD-MS: $m/z = 387.5$ (13%, M^{2+}), 620.7 (2%, $[M(\mathbf{1a})]^+$), 760.0 (23%, $[M - \text{CH}_3]^+$), 774.9 (100%, M^+), 1551.1 (3%, $[2M]^+$).

Compound 2b (macrocycle labelled with 4-amino-TEMPO)

N-Hydroxysuccinimide (12 mg, 0.11 mmol) was added to a suspension of macrocyclic acid **2a**¹³ (100 mg, 0.07 mmol) in CH_2Cl_2 (5 ml). After addition of *N,N'*-dicyclohexylcarbodiimide (23 mg, 0.11 mmol) the thick suspension was heated to 44 °C, whereupon it became a very faintly turbid solution. After stirring the reaction mixture at 44 °C for 25 min the heating bath was removed and 4-amino-TEMPO (26 mg, 0.15 mmol) was added to the solution at room temperature. The reddish brown, slightly turbid solution was stirred at room temperature for 44 h. Because the TLC (silica gel; petroleum ether/ CH_2Cl_2 /diethyl ether 15:15:2 v/v/v) suggested an incomplete reaction, the reaction mixture was heated again to 45 °C for 5.3 h, and afterwards kept for another 17 h at room temperature. Despite the longer reaction time, the TLC revealed no change in the product composition. The reaction mixture was filtered, the solid was washed with CH_2Cl_2 and the solvent was removed from the filtrate at reduced pressure. Chromatography using a chromatotron (the compound was applied as a solution in $\text{CH}_2\text{Cl}_2/\text{CHCl}_3$; elution with petroleum ether/ CH_2Cl_2 1:1 v/v \rightarrow petroleum ether/ $\text{CH}_2\text{Cl}_2/\text{Et}_2\text{O}$ 30:30:1 v/v/v \rightarrow 5:5:1 v/v/v) revealed **2b** (76 mg, 70%) to be a reddish solid. m.p. = 185 °C sintering with decomposition (most probably the transition into a liquid crystalline phase (Ref. 25); ^1H NMR: all signals are broad. $\delta = 7.86$ (very broad s, 2 H, H_α), 7.61 (apparent s, 8 H, H_β), 7.49 (half of AA'XX', 4 H, H_γ -2,-6), 7.41 and 7.33 (AA'XX', 4 H each, H_δ), 6.89 (half of AA'XX', 4 H, H_γ -3,-5), 4.00 (t, $J = 6.3$ Hz, 4 H, ArOCH_2), 3.21 (s, 3 H, OCH_3), 2.41 (t in outlines, 4 H, $\text{CH}_2\text{C}\equiv\text{C}$), 1.80 (m, 4 H, OCH_2CH_2), 1.60 (m, 4 H, $\text{CH}_2\text{CH}_2\text{C}\equiv\text{C}$), 1.6–1.2 (m, ca 82 H, CH_2 of macrocycle and protons of the spin label); elemental analysis (%) calculated for $\text{C}_{111}\text{H}_{139}\text{N}_2\text{O}_5$ (1581.342): C 84.31, H 8.86, N 1.77; found C 84.26, H 8.92, N 1.69. FD-MS: $m/z = 789.6$ (27%, M^{2+}), 1564.2 (47%, $[M - \text{CH}_3]^+$), 1578.9 (100%, M^+).

Compounds 3b and 3d-[2]catenane labelled once (3b) or twice (3d) with 4-amino-TEMPO

Statistical methylation of catenane diacid 3a. A solution of methyl iodide [0.42 ml of a solution of MeI (50 μl) in dry DMF (10 ml); 0.034 mmol] in DMF was added to a suspension of catenane diacid **3a**¹³ (96.8 mg, 0.034 mmol) and K_2CO_3 (9.3 mg, 0.07 mmol) in DMF (2 ml) and THF (2 ml). After stirring the reaction mixture at 44 °C for 16 h, it was cooled with an ice bath and 5 N HCl was added slowly. The yellow precipitate dissolved upon addition of CH_2Cl_2 . The aqueous phase was extracted with CH_2Cl_2 , the combined organic phases were washed initially with 2 N HCl and finally with water and were dried (Na_2SO_4). The solid obtained after removal of the solvent under reduced pressure contained a substantial amount of DMF. Therefore, the crude product was once again dissolved in a

mixture of CH_2Cl_2 and diethyl ether and this solution was washed extensively with water. Drying (Na_2SO_4) and removal of solvent gave a beige-coloured solid (94 mg) that was freeze-dried from benzene to remove residual solvents. ^1H NMR spectroscopy revealed a mixture of diacid **3a** and the corresponding monomethylester and dimethylester at the ratio of 1:2:1. ^1H -NMR: $\delta = 8.10$ (s, 2 H, H_α of the ring with the CO_2H group of the monoester), 8.09 (s, 4 H, H_α of diacid **3a**), 8.03 (s, 2 H of monoester and 4 H of diester, H_α of the ring with the CO_2Me group of mono ester and diester), 7.58, 7.57 (two apparent s, 16 H each, H_β), 7.45 (half of AA'XX', 8 H, H_γ -2,-6), 7.38 and 7.29 (AA'XX', 8 H each, H_δ), 6.85 (half of AA'XX', 8 H, H_γ -3,-5), 3.94 (t, $J = 6.5$ Hz, 8 H, ArOCH_2), 3.91 (s, 3 H of monoester and 6 H of diester, CO_2CH_3), 3.183, 3.175, 3.166 (3 s, 6 H each, ArOCH_3), 2.37 (t, $J = 7.0$ Hz, 8 H, $\text{CH}_2\text{C}\equiv\text{C}$), 1.76 (m, 8 H, OCH_2CH_2), 1.56 (m, 8 H, $\text{CH}_2\text{CH}_2\text{C}\equiv\text{C}$), 1.5–1.2 (m, 152 H, CH_2); Mixture of $\text{C}_{204}\text{H}_{244}\text{O}_{10}$ (2856.186), $\text{C}_{205}\text{H}_{246}\text{O}_{10}$ (2870.213), $\text{C}_{206}\text{H}_{248}\text{O}_{10}$ (2884.240): MALDI-TOF (dithranol): $m/z = 2856.5$ (37%, $[M_{\text{H,H}}]^+$), 2871.5 (56%, $[M_{\text{H,Me}}]^+$), 2885.5 (12%, $[M_{\text{Me,Me}}]^+$), 2879.3 (41%, $[M_{\text{H,H}} + \text{Na}]^+$), 2893.3 (31%, $[M_{\text{H,Me}} + \text{Na}]^+$), 2908.4 (23%, $[M_{\text{Me,Me}} + \text{Na}]^+$).

Labelling of the catenane with 4-amino-TEMPO. *N*-Hydroxysuccinimide (4.9 mg, 0.04 mmol) and *N,N'*-dicyclohexylcarbodiimide (9.0 mg, 0.04 mmol) were subsequently added to a solution of the obtained mixture (86.8 mg, 0.03 mmol carboxyl groups) of catenane diacid and its corresponding monomethylester and dimethylester in CH_2Cl_2 (4 ml). The reaction mixture was stirred at 45 °C for 30 min. After removal of the heating bath, 4-amino-TEMPO (12.0 mg, 0.07 mmol) was added to the solution at room temperature. The solution turned turbid. After stirring the suspension for 20 h at room temperature, it was filtered, the precipitate was washed with CH_2Cl_2 and the solvent of the filtrate was removed under reduced pressure. The products were separated through chromatography using a chromatotron. Elution with petroleum ether/ CH_2Cl_2 1:1 v/v gave catenane dimethylester (19 mg, 21% over two steps) as a colourless solid; further elution with petroleum ether/ $\text{CH}_2\text{Cl}_2/\text{Et}_2\text{O}$ 30:30:1 \rightarrow 15:15:2 v/v/v gave mono-labelled [2]catenane **3b** (32 mg, 34% over two steps) as a beige-coloured solid and finally elution with petroleum ether/ $\text{CH}_2\text{Cl}_2/\text{Et}_2\text{O}$ 2:2:1 v/v/v gave doubly labelled [2]catenane **3d** (11 mg, 11% over two steps) as a slightly reddish solid. The products were freeze dried from benzene.

Analytical data for mono-labelled [2]catenane 3b

m.p. = 110.2–111.3 °C; ^1H NMR: All signals are broad. $\delta = 8.04$ (s, 2 H, H_α of macrocycle with the ester group), 7.8 (very broad s, H_α of macrocycle with the amide group), 7.58 (apparent s, 16 H, H_β), 7.46 (half of AA'XX', 8 H, H_γ -2,-6), 7.39 and 7.30 (AA'XX', 8 H each, H_δ), 6.86 (half of AA'XX', 8 H, H_γ -3,-5), 3.96 (t, $J = 6.4$ Hz, 8 H, ArOCH_2), 3.92 (s, 3 H, CO_2CH_3), 3.18 (s, 6 H, ArOCH_3), 2.38 (t, $J = 6.8$ Hz, 8 H, $\text{CH}_2\text{C}\equiv\text{C}$), 1.77 (m, 8 H, OCH_2CH_2), 1.58 (m, 8 H, $\text{CH}_2\text{CH}_2\text{C}\equiv\text{C}$), 1.5–1.2 (m, ca 163 H, CH_2 of macrocycle and protons of the spin label); elemental analysis (%) calculated for $\text{C}_{214}\text{H}_{263}\text{N}_2\text{O}_{10}$ (3023.462): C 85.01, H 8.77, N 0.93; found C 84.68, H 8.66, N 0.84. MALDI-TOF (Dithranol, KO_2CCF_3): $m/z = 3025$ (8%, M^+), 3063 (16%, $[M + \text{K}]^+$).

Analytical data for doubly labelled [2]catenane 3d

^1H NMR: all signals are broad and the fine structures are hardly resolved. $\delta = 7.57$ (apparent s, ca 16 H, H_β ; most probably overlapping with signal of H_α), 7.45 (half of AA'XX', 8 H, H_γ -2,-6), 7.38 and 7.30 (AA'XX', 8 H each, H_δ), 6.85 (half of AA'XX', 8 H, H_γ -3,-5), 3.96 (t in outlines, 8 H, ArOCH_2), 3.48 (s, signal of unknown impurity), 3.16 (s, 6 H, ArOCH_3), 2.38 (t in outlines, 8 H, $\text{CH}_2\text{C}\equiv\text{C}$), 1.92 (m, signal of unknown impurity), 1.8–1.2 (m, ca 189 H, CH_2 of macrocycle and protons of the spin label); $\text{C}_{222}\text{H}_{278}\text{N}_4\text{O}_{10}$ (3162.684): MALDI-TOF (dithranol, KO_2CCF_3): $m/z = 3165$ (4%, M^+), 3202 (8%, $[M + \text{K}]^+$).

Acknowledgements

The authors thank Deutsche Forschungsgemeinschaft for financial support within SPP 1051 (Hochfeld-EPR), Michael Mehring for helpful discussions, Christian Bauer for technical support and Jürgen Thiel for assistance during the synthesis.

REFERENCES

1. Steed JW, Atwood JL. *Supramolecular Chemistry*. Wiley: Chichester, 2000.

2. (a) Sauvage JP. *Acc. Chem. Res.* 1998; **31**: 611; (b) Colassen BX, Dietrich-Buchecker C, Jimenez-Molero MC, Sauvage JP. *J. Phys. Org. Chem.* 2002; **15**: 476.
3. (a) Balzani V, Credi A, Raymo FM, Stoddart JF. *Angew. Chem.* 2000; **112**: 3483; (b) Balzani V, Credi A, Raymo FM, Stoddart SF. *Angew. Chem., Int. Ed. Engl.* 2000; **39**: 3348; (c) Balzani V, Venturi M, Credi A. *Molecular Devices and Machines: A Journey into the Nanoworld*. Wiley-VCH: Weinheim, 2003; (d) Pease AR, Jeppesen JO, Stoddart JF, Luo Y, Collier CP, Heath JR. *Acc. Chem. Res.* 2001; **34**: 433.
4. (a) Leigh DA, Wong JKY, Dehez F, Zerbetto F. *Nature* 2003; **424**: 174; (b) Bottari G, Dehez F, Leigh DA, Nash PJ, Pérez EM, Wong JKY, Zerbetto F. *Angew. Chem.* 2003; **115**: 6066; (c) Bottari G, Dehez F, Leigh DA, Nash PJ, Pérez EM, Wong JKY, Zerbetto F. *Angew. Chem., Int. Ed. Engl.* 2003; **42**: 5886; (d) Raymo FM. *Adv. Mater.* 2002; **14**: 401.
5. Schalley CA, Beizai K, Vögtle F. *Acc. Chem. Res.* 2001; **34**: 465.
6. (a) Vaia RA, Dudis D, Henes J. *Polymer* 1998; **39**: 6021; (b) Farmer BL, Chapman BR, Dudis DS, Adams WW. *Polymer* 1993; **34**: 1588.
7. Godt A. *Eur. J. Org. Chem.* 2004; **8**: 1630.
8. Schmidt-Rohr K, Spiess HW. *Multi-Dimensional Solid-State NMR and Polymers*. Academic Press: London, 1994.
9. Berliner LJ (ed). *Biological Magnetic Resonance, vol. 14: Spin Labeling: The Next Millenium*. Plenum Press: New York, 1998.
10. Milov AD, Salikhov KM, Shirov MD. *Fiz. Tverd. Tela (Leningrad)* 1981; **23**: 957.
11. Jeschke G, Koch A, Jonas U, Godt A. *J. Magn. Reson.* 2002; **155**: 72.
12. Jeschke G, Panek G, Godt A, Bender A, Paulsen H. *Appl. Magn. Reson.* 2004; **26**: 223.
13. Jeschke G, Godt A. *Chemphyschem* 2003; **4**: 1328.
14. Ünsal O, Godt A. *Chem. Eur. J.* 1999; **5**: 1728.
15. Schneider DJ, Freed JH. In *Biological Magnetic Resonance*, vol. 8, Berliner LJ, Reuben J (eds). Plenum Press: New York, 1989; 1.
16. Liang Z, Freed JH. *J. Phys. Chem. B* 1999; **103**: 6384.
17. Steinhoff HJ, Hubbell WL. *Biophys. J.* 1996; **71**: 2201.
18. Eviatar H, VanFassen EE, Levine YK, Hoult DI. *Chem. Phys.* 1994; **181**: 369.
19. Buchachenko AL, Kovarskii AL, Vasserman AM. In *Advances in Polymer Science*, Rogovin ZA (ed). Wiley: New York, 1974; 26.
20. Molin YN, Salikhov KM, Zamaraev KI. *Spin Exchange*. Springer: Berlin, 1980.
21. Hinderberger D, Spiess HW, Jeschke G. *Europhys. Lett.* 2005; **70**: 102.
22. Hanke A, Metzler R. *Chem. Phys. Lett.* 2002; **359**: 22.
23. Godt A, Ünsal O, Roos M. *J. Org. Chem.* 2000; **65**: 2837.
24. Godt A. *J. Org. Chem.* 1997; **62**: 7471.
25. Duda S, Godt A. *Eur. J. Org. Chem.* 2003; 3412.